# Assessment of diffusive isotopic fractionation in polar firn, and application to ice core trace gas records

Christo Buizert[a,b], Todd Sowers[c], Thomas Blunier[b]

[a]College of Earth, Ocean, and Atmospheric Sciences, 104 CEOAS Admin Bldg, Oregon State University, Corvallis, OR 97331-5503, USA
[b]Centre for Ice and Climate, Niels Bohr Institute, University of Copenhagen, Juliane Maries vej 30, DK-2100 Copenhagen Ø, Denmark
[c]The Earth and Environmental Systems Institute, Penn State University, 317B EESB Building, University Park, PA 16802, USA

## Abstract

During rapid variations of the atmospheric mixing ratio of a trace gas, diffusive transport in the porous firn layer atop ice sheets and glaciers alters the isotopic composition of that gas relative to the overlying atmosphere. Records of past atmospheric trace gas isotopic composition from ice cores and firn need to be corrected for this diffusive fractionation artifact.

We present a novel, semi-empirical method to accurately estimate the magnitude of the diffusive fractionation in the ice core record. Our method (1) consists of a relatively simple analytical calculation; (2) requires only commonly available ice core data; (3) is not subject to the uncertainties inherent to estimating the accumulation rate, temperature, close-off depth and depth-diffusivity relationship back in time; (4) does not require knowledge of the true atmospheric variations, but uses the smoothed records obtained from ice cores; (5) arguably gives more accurate results than a combined firn densification–firn air transport modeling study would.

We apply the method to records of $CH_4$, $CO_2$ and $N_2O$ mixing ratios,

and we find that the correction is particularly important for $\delta^{13}C-CH_4$. We apply the correction to $\delta^{13}C-CH_4$ records over the last glacial termination and the 8.2 ka event. In both cases the diffusive signal exceeds the analytical precision of the data, and has a significant impact on the observed isotopic trends. For the 8.2 ka event the corrected data show an isotopic enrichment in $\delta^{13}C-CH_4$ for the duration of the event, consistent with reduced wetland emissions.

## 1. Introduction

Ice core records of the isotopic composition of trace gas species provide fundamental boundary constraints for understanding past changes in biogeochemical cycles and their relation to climate change (Bock et al., 2010b; Fischer et al., 2008; Lourantou et al., 2010; Schmitt et al., 2012; Sowers et al., 2003; Sowers, 2006, 2010). The important greenhouse gases $CO_2$, $CH_4$ and $N_2O$ all show variations in their atmospheric mixing ratio on the orbital timescales of glacial cycles, as well as rapid millennial scale variations associated with Dansgaard-Oeschger (DO) interstadials (Lüthi et al., 2008; Loulergue et al., 2008; Schilt et al., 2010). Records of the isotopic composition of these gases can help to identify past changes in the atmospheric budget that caused the observed variations.

The different isotopologues of a trace gas have different masses, and therefore they diffuse at slightly different rates through the firn layer (the porous 50-100 m thick perennial snowpack on top of ice sheets and glaciers). Dur-

2

ing a rapid change in atmospheric mixing ratio, this difference in diffusivity leads to an isotopic fractionation of the gas mixture in the firn relative to the overlying atmosphere (Trudinger et al., 1997). For example, the heavier $^{13}CO_2$ isotopologue diffuses more slowly into the firn than $^{12}CO_2$, leading to a deep firn depletion (enrichment) in $\delta^{13}C$ during an increase (decrease) in atmospheric $CO_2$ mixing ratio. This so-called diffusive fractionation (DF) occurs only when the atmospheric mixing ratio of a trace gas is changing with time.

Firn air records of isotopic composition are routinely corrected for the effects of DF. When the gas transport properties of a firn site are well characterized using reference tracers (Trudinger et al., 1997; Rommelaere et al., 1997), the DF correction can be calculated using a firn air transport model assuming known diffusion coefficients. In this way the maximum DF correction during the recent anthropogenic increase was found to be $\sim 0.1\,\permil$ for $\delta^{13}C$–$CO_2$ at DE08, Law Dome (Francey et al., 1999) and $1.2\,\permil$ for $\delta^{13}C$–$CH_4$ at WAIS-Divide (Mischler et al., 2009). The DF correction is both time- and site-specific, and needs to be calculated individually for each sample. A recent study compares DF calculated by six different firn air models, showing good model agreement in the upper firn where diffusion dominates the transport. However, the models diverge in the lock-in zone where gas transport is dominated by downward advection with the ice matrix (Buizert et al., 2012).

Because gas bubbles are occluded at the bottom of the firn column, ice core records of trace gas isotopic composition (such as e.g. $\delta^{13}C$–$CO_2$ or $\delta^{13}C$–$CH_4$) should also be corrected for the effects of DF. A complete de-

scription of the problem requires two things. First, using a dynamical firn densification model, the firn density profile and close-off depth need to be reconstructed back in time (Goujon et al., 2003; Barnola et al., 1991). The densification modeling requires reconstructed past accumulation rates and temperatures as an input. Second, the movement of trace gases in the firn needs to be modeled using a firn air transport model. This second modeling step requires knowledge of the effective gas diffusivity with depth, which can only be obtained from density–diffusivity parameterizations (Schwander, 1989; Freitag et al., 2002). These parameterizations are based on transport modeling or diffusivity measurements on finite-size firn samples; the results do not adequately represent the transport properties of the entire firn pack, which are in part controlled by macro-scale features such as layering (Fabre et al., 2000). The fit obtained to experimental data using diffusivity parameterizations is generally not very good.

Such a combined firn densification–firn air transport modeling approach requires considerable effort, and is subject to uncertainties in reconstructed temperatures, accumulation rates and firn properties, as well as the aforementioned uncertainty in the diffusivity parameterization. Here we present an alternative method for DF correction that is simple to implement, computationally inexpensive, and not subject to as many uncertainties.

First we present an analytical expression for DF in the firn column, which provides new insights into the nature of this phenomenon. Using ten well-characterized firn air sites, we find an empirical expression for the gas age at the lock-in depth. On combining these two results, we have a convenient

4

framework for estimating DF throughout an ice core record. We test the accuracy and dynamic response of our method by comparing it to a full firn air transport model forced with atmospheric signals at different time scales. Using ice core records of $CO_2$, $CH_4$ and $N_2O$ mixing ratios from both Greenland and Antarctica, we calculate the magnitude of the DF correction for the recent anthropogenic increase, glacial terminations I-III and for DO cycles during the previous glacial period. Finally we apply our methodology to $\delta^{13}C$–$CH_4$ records over the last glacial termination and the 8.2 ka event.

## 2. Analytical description of diffusive fractionation

For a linear increase or decrease in the atmospheric mixing ratio of a trace gas, we can derive a simple analytical expression for the DF. We assume an atmospheric forcing of the form

$$C = C_0 + kt \tag{1}$$

where $C$ is the mixing ratio of the major isotopologue in ppm or ppb, $k$ is the annual rate of growth or decrease in ppm $a^{-1}$ or ppb $a^{-1}$ and $t$ is the time in years. In the supplementary material we show that for this simplified forcing the diffusive fractionation in the firn $\varepsilon_{\mathrm{DF}}(z)$ is well approximated by

$$\varepsilon_{\mathrm{DF}}(z) \approx -\frac{k}{C}\left(\frac{D}{D_i} - 1\right)\Gamma(z) \times 10^3\ \text{‰} \tag{2}$$

where $D$ and $D_i$ are the free-air diffusivities of respectively the major and the minor isotopologue in $m^2\ a^{-1}$, and $\Gamma(z)$ is the mean gas age at depth $z$. Equation (2) is valid in the case $k\Gamma \ll C$. Strictly speaking $C$ refers to the major isotopologue only. For the trace gases considered here, the

5

major isotopologue is much more abundant ($\geq 99\%$) than the minor ones; for simplicity we will therefore assume $C$ to be identical to the atmospheric mixing ratio of the trace gas itself in the remainder of this work. Real atmospheric forcings will never be perfectly linear; still on the timescale of firn gas transport ($\Gamma \sim 10\text{–}25$ years) they can be well approximated by a linear slope. Note that the gas age $\Gamma(z)$ denotes the average time it takes a gas molecule to reach depth $z$ after it crossed the atmosphere-firn interface, and not the age of the gas in years before present.

From Eq. (2) we can draw a number of interesting conclusions. First, it is not the increase $k$ itself that matters, but rather the relative increase $k/C$. Second, the DF scales linearly with $(D/D_i - 1)$. This quantity is shown in Table 1 for several trace gases relevant to ice core studies, and is largest for light gases such as $CH_4$ and $H_2$. Because these molecules have low molecular weights ($M_{CH_4} = 16.04$ kg mol$^{-1}$ and $M_{H_2} = 2.02$ kg mol$^{-1}$), introducing an additional neutron to the atomic nucleus presents a larger fractional change in the total weight compared to molecules with higher molecular weights. Third, the DF scales linearly with the age of the gas. The gas age at the firn-ice transition (where the air is trapped) is primarily dependent on the depth of the firn-ice transition. DF is therefore larger at Antarctic plateau sites than in (warmer) coastal and Greenlandic sites. Fourth, as both isotopologues diffuse through the same firn column, the exact shape of the depth-diffusivity profile (i.e. the tortuosity) does not matter. The ratio of molecular diffusivities is constant throughout the firn column irrespective of the pore structure.

6

The result of Eq. (2) is valid only in the diffusive zone (DZ) where advection is negligible. In the lock-in zone (LIZ) advection dominates the gas transport. Advection does not discriminate between isotopologues, giving no continued fractionation with depth. For this reason the fractionation $\varepsilon_{\mathrm{DF}}$ along the entire firn column is well approximated by

$$\varepsilon_{\mathrm{DF}} = \begin{cases} -\frac{k}{C}\left(\frac{D}{D_i} - 1\right)\Gamma(z) \times 10^3 \; \permil & \text{for} \quad z \leq z_{\mathrm{lid}} \\ -\frac{k}{C}\left(\frac{D}{D_i} - 1\right)\Gamma(z_{\mathrm{lid}}) \times 10^3 \; \permil & \text{for} \quad z > z_{\mathrm{lid}} \end{cases} \tag{3}$$

with $z_{\mathrm{lid}}$ representing the lock-in depth separating the DZ and LIZ. In Fig. 1 the output of six firn air transport models is compared to Eq. (3) for the NEEM site in Northern Greenland. The models use a hypothetical atmospheric forcing of exponentially increasing $CO_2$ mixing ratio ($k/C = 2.5 \cdot 10^{-3}$ a$^{-1}$). We find that within the DZ our analytical expression agrees very well with the model results within about 5% difference. The analytical curve is not completely independent from the firn models, though, given that the modeled gas age $\Gamma(z)$ is used as an input. Still, the good agreement confirms the validity of Eq. (2). Upon reaching the LIZ, the model solutions diverge strongly; our solution falls within the model solution envelope. We conclude that Eq. (3) gives an accurate prediction of $\varepsilon_{\mathrm{DF}}$ in the firn.

The observed spread in model results is due to differences in the way the models parameterize LIZ mixing (Buizert et al., 2012). Although the absence of gravitational enrichment argues against a dominance of diffusive transport in the LIZ, some diffusion (and thereby continued fractionation) cannot be excluded. Until we know which of the models predicts $\varepsilon_{\mathrm{DF}}$ correctly, an additional uncertainty needs to be ascribed to any $\varepsilon_{\mathrm{DF}}$ estimate to account

for the observed model divergence. In the deepest firn the $1\sigma$ uncertainty is around 15% of the modeled $\varepsilon_{DF}$ value.

## 3. Parameterizing gas age at the lock-in depth

All of the bubble trapping occurs either within, or just above, the LIZ (Battle et al., 2011). The value of $\varepsilon_{DF}$ at $z_{lid}$ will therefore represent the $\varepsilon_{DF}$ as recorded in the ice. Equation (2) allows us to calculate $\varepsilon_{DF}$ in the ice core record in order to correct isotopic measurements; $C$ and $k$ can be derived from measured trace gas mixing ratios, the lock-in depth gas age $\Gamma(z_{lid})$ is the only unknown. Here we derive an empirical parameterization of $\Gamma(z_{lid})$.

We tune the CIC firn air model (Buizert et al., 2012) to ten firn air sites, representing both hemispheres and a wide range of climatic conditions ($0.025 \leq A \leq 1.2$ m ice a$^{-1}$ and $-54 \leq T \leq -19\,°C$). The site characteristics are summarized in Table 2. For each site we reconstruct the diffusivity-depth profile using reference tracers of known atmospheric history (supplement). Details of firn air data and sampling are described elsewhere (Atlas et al., a,b; Battle et al., 1996, 2011; Etheridge et al., 1996; Sturrock et al., 2002; Ishijima et al., 2007; Severinghaus et al., 2010; Witrant et al., 2011; Buizert et al., 2012). For our purpose we define $z_{lid}$ as the depth where the tortuosity of the pore geometry reduces the effective molecular diffusivity to one thousandth of the free air diffusivity; typically this is equal to the depth where gravitational enrichment ceases, but easier to calculate in a consistent manner (for several sites $\delta^{15}N$–$N_2$ data are either not available or of poor quality).

The mean gas age $\Gamma_X(z_{lid})$ of gas $X$ depends primarily on the depth $z_{lid}$, the firn tortuosity profile, and the free air diffusivity of the gas. The latter

is given (in m$^2$ a$^{-1}$) following (Schwander et al., 1988; Buizert et al., 2012):

$$D_X^0 = \gamma_X \frac{1013.25}{p} \times 1.81 \cdot 10^{-2} \, T^{1.81} \tag{4}$$

where $\gamma_X = D_X/D_{CO_2}$ is the free air diffusivity relative to $CO_2$ (Table 1), $p$ the site atmospheric pressure in hPa, and $T$ the absolute temperature in K. At each of the ten sites we model the transport of the trace gases $CH_4$, $CO_2$, and a third (hypothetical) trace gas with $\gamma_X = 0.75$ to broaden the $\gamma_X$-range. In Fig. 2 we plot the modeled $\Gamma(z_{lid})$ versus the following parameterization:

$$\Gamma_X(z_{lid}) = \frac{1}{\gamma_X} \left( 0.934 \cdot \frac{DCH^2}{D_{CO_2}^0} + 4.05 \right) \tag{5}$$

with DCH the diffusive column height. Note that $D_{CO_2}^0$ must be expressed in units of m$^2$ a$^{-1}$ to obtain a gas age in years. The reciprocal of $\gamma_X$ in Eq. (5) ensures that at a given site the gas age scales inversely with the diffusion coefficient, as required by Fick's second law; the term in parentheses describes how firn dimensions and climatic conditions influence the gas age. Diffusive transport through a homogeneous medium (constant $D$) would yield a linear scaling between $\Gamma$ and $DCH^2$. Instead, in polar firn the effective diffusivity decreases strongly with depth. This results in an age offset in Eq. (5) of 4.05 years for $CO_2$, leading to the unphysical result that $\Gamma$ does not go to zero in the limit $DCH \to 0$. Therefore Eq. (5) should be used with caution outside of the DCH range used in the calibration ($36 \leq DCH \leq 115$ m).

There are good reasons for using the DCH rather than the lock-in depth itself in the age parameterization. First, paleo DCH values can directly be obtained from ice core measurements of $\delta^{15}N$–$N_2$ or $\delta^{40}Ar$. The lock-in depth, on the other hand, needs to be reconstructed using firn densification models.

Second, vigorous ventilation in the upper firn has the effect of reducing the mean gas age in the pores. While the influence of this process diminishes strongly with depth, the near surface convective zone thickness is a reliable measure of its impact on firn air transport. Consequently the DCH is more representative of the effective diffusive path length than the lock-in depth. In particular the good fit of the anomalous Megadunes site, where deep surface cracks facilitate a 23 m deep convective zone (Severinghaus et al., 2010), supports the idea that it is the DCH rather than the lock-in depth that controls the gas age.

The age parameterization of Eq. (5) can also be used when modeling $\Delta$age back in time (e.g. Schwander et al., 1997). The ice age at gas lock-in can be calculated with a firn densification model, yet to obtain $\Delta$age the gas age should be subtracted. As the details of the paleo diffusivity-depth profile are unknown, Eq. (5) can be used to calculate the age based on the DCH alone. It must be noted, though, that the error in $\Delta$age calculations primarily comes from the uncertainty in estimating the ice age.

## 4. Diffusive fractionation in the ice core record

### 4.1. Methodology

Equations (2) and (5) together provide a simple method to calculate $\varepsilon_{\mathrm{DF}}$ in the ice core record. The method consists of three steps. A calculation example is given in the supplement. The first step is to estimate DCH from $\delta_{\mathrm{grav}}$, the gravitational enrichment per unit mass. The DCH is given by $\mathrm{DCH} = \ln\left(\delta_{\mathrm{grav}}/10^3 + 1\right) \times RT/\Delta M g$, where $\Delta M$ is the unit mass difference $\Delta M = 1 \cdot 10^{-3}$ kg mol$^{-1}$. For Greenland, interpretation is complicated by the

presence of transient isotopic signals caused by rapid temperature variations (Severinghaus and Brook, 1999; Leuenberger et al., 1999). In Antarctica, climate-induced temperature changes are too gradual to impose large transient thermal signals; however, the low accumulation rates there can cause the geothermal gradient to extend up into the firn column, reducing $\delta^{15}$N–N$_2$ slightly below $\delta_{\text{grav}}$ (Goujon et al., 2003). When available, one should use $\delta_{\text{grav}}$ records corrected for thermal effects, either by modeling or through simultaneous measurements of $\delta^{15}$N–N$_2$ and $\delta^{40}$Ar. The error made when using uncorrected $\delta^{15}$N–N$_2$ data for DF correction is estimated in Section 5. The second step is to use the DCH estimate and $D_X^0$ to calculate $\Gamma_X(z_{\text{lid}})$. The variations in temperature and pressure caused by changing climate and surface elevation have a limited impact on $D_X^0$, and can be included or neglected as desired. The third step is to derive $C$ and $k$ from ice core time series, and combine them with $\Gamma_X(z_{\text{lid}})$ in Eq. (2) to calculate $\varepsilon_{\text{DF}}$. Here $k = dC/dt$ is the trend of the ice core time series at a given gas age.

To test the accuracy and dynamic response of our method, we compare it to the output of the firn air model under known (i.e. modern) firn conditions. We test two different atmospheric variations: a ramp and a Gaussian curve, the duration/width of which is varied from 1, 10, 100 to 1000 years. For both NEEM and South Pole, $\varepsilon_{\text{DF}}$ is calculated for $\delta^{13}$C–CH$_4$ and $\delta^{13}$C–CO$_2$. In the supplement we show that for both gases and at both sites, our method agrees with the firn air model within the LIZ transport uncertainty described in Section 2. We also observe that the $\varepsilon_{\text{DF}}$ signal is smoothed in the firn to the same degree as the mixing ratio signal. Consequently $C$ and $k$ values are

ideally obtained from the same ice core as the isotopic measurements. Also, the mixing ratio records should not be corrected for firn smoothing using deconvolution schemes (Spahni et al., 2003; Köhler et al., 2011).

Our method requires taking the derivative $k = dC/dt$, which is complicated by the fact that ice core time series are not equitemporally spaced and subject to noise. How the derivatives were taken for the records presented in this paper is outlined in the supplement. Due to recent technological advances, continuous methane records are becoming available (Schüpbach et al., 2009; Stowasser et al., 2012). Continuous records do not suffer from aliasing due to undersampling of the atmospheric signal, making trend estimation more reliable (assuming unchanged measurement precision).

*4.2. Diffusive fractionation during rapid atmospheric changes*

We now apply our method to ice core time series to calculate $\varepsilon_{\mathrm{DF}}$ for past atmospheric variations. The results are shown in Fig. 3 for Greenland (GISP2 and NGRIP), and Fig. 4 for Antarctica (EPICA Dome C). Typical values of the DF correction for the anthropogenic increase, glacial terminations and DO cycles are listed in Table 3; note that the values are site dependent. Because the signals for $N_2O$ are generally small, they are not shown in Figures 3 and 4, but only listed in Table 3. In the calculations the DCH is based on $\delta_{\mathrm{grav}}$ rather than $\delta^{15}N$–$N_2$ itself. For $CH_4$, the DF is effectively identical for $\delta^{13}C$ and $\delta D$ ($=\delta^2H$) (difference $< 0.005\,‰$), and therefore only $\delta^{13}C$–$CH_4$ is shown.

The DF correction becomes relevant whenever $\varepsilon_{\mathrm{DF}}$ is comparable to, or greater than the analytical precision of the isotopic data. In Table 3 we list typical values of $\varepsilon_{\mathrm{DF}}$ for rapid atmospheric variations (the anthropogenic in-

12

crease, the last three glacial terminations, and DO cycles), together with the reported precision range of analytical setups.

It is clear that for methane the diffusive effect is strongest. This is in part because of the small molecular mass, which leads to a large difference between the isotopologue diffusion coefficients. Also, because of its short atmospheric residence time, the $CH_4$ mixing ratio can change very rapidly. The methane record shows the most abrupt changes of all atmospheric trace gases. The magnitude of $\varepsilon_{DF}$ is identical for both $\delta^{13}C$ and $\delta D$ of $CH_4$, yet the need for data correction is different. For $\delta^{13}C$ the DF correction exceeds the analytical precision for all the rapid atmospheric signals considered here, while for $\delta D$ the DF correction will typically be below the measurement uncertainty. Consequently all $\delta^{13}C$–$CH_4$ data during rapid $CH_4$ variations should be DF corrected, while one could justify omitting the DF correction for $\delta D$–$CH_4$. The $-1‰$ $\delta^{13}C$–$CH_4$ fractionation we find at GISP2 for the YD termination at 11.7 ka BP is comparable to the -0.75‰ calculated with a firn diffusion model for the Pâkitsoq ice margin in West Greenland (Melton et al., 2012). As the correction is site specific, such differences are to be expected.

Nitrous oxide provides a simple case. With the exception of the anthropogenic signal, the DF correction is more than an order of magnitude smaller than the analytical precision and can safely be neglected. The case of $CO_2$ is similar. However, because the analytical precision is so much better for $\delta^{13}CO_2$, one could consider applying the DF correction during the deglaciations, which are accompanied by a relatively strong $CO_2$ increase.

13

For all trace gases considered, the largest fractionation is obtained for the current anthropogenic increase, showing the profound impact mankind has on the chemical composition of our atmosphere. The anthropogenic signal is found in the firn or shallow ice, rather than in the deep core. For firn air measurements the analytical precision will be better than the values listed in Table 3, as sample sizes are larger and no ice extraction step is needed. For all firn air trace gases a DF correction is therefore required. In the firn, $\varepsilon_{DF}$ can also be estimated using a firn air transport model. When the firn air model is well calibrated using reference tracers, this gives more accurate results than our method does. Note that the values listed in Table 3 correspond to the most rapid increases; $\varepsilon_{DF}$ varies throughout the anthropogenic era.

In summary, $\delta^{13}C$–$CH_4$ is the only trace gas isotopic signal for which the DF correction should always be applied during transitions. Firn air data for all trace gases covering the anthropogenic increase should also be corrected for DF. For $\delta D$–$CH_4$ and $\delta^{13}C$–$CO_2$ the magnitude of $\varepsilon_{DF}$ gets to about half the analytical precision only during glacial terminations; one could consider DF correction during these special intervals. In all other cases the effects of DF can safely be neglected. We believe that the method presented here also has merits in cases where $\varepsilon_{DF}$ is very small. With our method, the magnitude of $\varepsilon_{DF}$ can be estimated with little effort, enabling experimentalists to quickly asses whether or not they need to worry about DF correcting their data.

*4.3. Correcting $\delta^{13}C$–$CH_4$ data for DF*

Here we correct published records of $\delta^{13}C$–$CH_4$ over the last glacial termination (Fischer et al., 2008) and the 8.2 ka event (Sowers, 2010) for the effect of DF. For the last termination the results are shown in Fig. 5c, with the original (uncorrected) data in blue and the DF corrected data in orange. During each rapid variation in atmospheric $CH_4$ (indicated by grey shading), we find a substantial DF signal. For the three transitions the correction ranged from 0.30–0.53 ‰, which is more than double the analytical precision of 0.15 ‰ in the study. The errorbars on the corrected data include the uncertainty in our method, which we estimate in section 5.1. As we do not know the original atmospheric $\delta^{13}C$–$CH_4$, we can not provide conclusive proof for the correctness of our method. Having said this, we do believe that the corrected dataset is more consistent with the $CH_4$ mixing ratios. The Younger-Dryas to Preboreal (YD-PB) transition at 11.7 ka BP shows a remarkable isotopic reversal in the uncorrected dataset. With the correction this prominent feature disappears, giving an intuitively more realistic monotonic rise in $\delta^{13}C$–$CH_4$. Also the transition from the Oldest Dryas into the Bølling interstadial (14.8 ka BP) arguably looks more realistic after DF correction, with the isotopes following the atmospheric $CH_4$ signal more closely.

The 8.2 ka event is an abrupt climate event within the climatically stable Holocene, which brought dry and cold conditions to large regions of the Northern hemisphere (Alley and Ágústsdóttir, 2005). It has been attributed to a freshening of the North Atlantic by an outburst flood, slowing down the

meridional circulation that transports heat northwards from lower latitudes. The 8.2 ka event shows a very prominent and abrupt $CH_4$ response (Spahni et al., 2003; Kobashi et al., 2007). This rapid variation leads to a large $\varepsilon_{DF}$, as shown in Fig. 6c, again with the original (uncorrected) data in blue and the DF corrected data in orange. The DF correction is on the same order of magnitude as the analytical precision, which is around 0.3 ‰ for this study. We reject one datapoint as an outlier (shown in grey). Including this datapoint would imply that within less than 30 years the isotopic composition jumped by nearly a per mil and back again; such a rapid variation is incompatible with the diffusive smoothing of the firn, and therefore certainly not of atmospheric origin.

After the correction we observe an enrichment in $\delta^{13}C$–$CH_4$ for the duration of the event, which hints at reduced wetland emissions under colder and dryer climatic conditions. Based on atmospheric budget considerations one would expect a close coupling between $CH_4$ mixing ratios and $\delta^{13}C$. Indeed, the DF-corrected isotopic record, like the $CH_4$ mixing ratio, shows a single excursion. By contrast, the uncorrected $\delta^{13}C$ time series shows two separated isotopic events without counterpart in the $CH_4$ record. To place the magnitude of the 8.2 ka $\delta^{13}C$–$CH_4$ signal in perspective, we draw an analog to the YD inception which also coincided with a sudden reduction in the Atlantic overturning circulation (McManus et al., 2004). The 180 ppb $CH_4$ drop from the Allerød to the YD was accompanied by a 1.5 ‰ enrichment in $\delta^{13}C$ ($-8.3$ per Meg ppb$^{-1}$); by comparison we find a $\sim$0.6 ‰ enrichment for a 75 ppb $CH_4$ drop during the 8.2 ka event ($-8.0$ per Meg ppb$^{-1}$). The similar ratio of $\delta^{13}C$–$CH_4$ to $CH_4$ amplitudes suggests that both climatic events had

a similar impact on the methane budget.

## 5. Discussion

### 5.1. The accuracy of our method

Here we will estimate the uncertainty in our method. We distinguish three major sources of uncertainty:

**1) The DCH estimate based on $\delta^{15}$N–N$_2$ data**. The analytical precision of the $\delta^{15}$N measurements is on the order of 0.005–0.01 ‰ (Dreyfus et al., 2010); since the depth coverage is not always equally good for each ice core, we estimate the uncertainty at 0.02 ‰ (corresponding to a DCH error of 4 m). More problematic is the possibility of thermal fractionation in the firn column caused by temperature gradients (Severinghaus et al., 2001), giving rise to transient excursions in $\delta^{15}$N–N$_2$ that do not reflect changes in the DCH (Severinghaus and Brook, 1999). These can be seen in in Fig. 3c, where we plot measured $\delta^{15}$N–N$_2$ data in red, and a reconstructed gravitational signal $\delta_{\mathrm{grav}}$ representing the DCH in black (Huber et al., 2006). In Antarctica temperature variations are generally too gradual to impose large gradients in the firn.

The measured $\delta^{15}$N–N$_2$ can be split into a gravitational and a thermal component: $\delta^{15}$N $= \delta_{\mathrm{grav}} + \delta_{\mathrm{therm}}$; if $\delta_{\mathrm{therm}}$ is not known an error is introduced. We estimate this maximum error from the difference between the apparent and true DCH in the Huber et al. (2006) study, i.e. the red and black curves in Fig. 3c. We disregard the rapid isotope excursions themselves as they are easily identified as thermal signals, and take the root mean square (RMS) of the remaining $\delta_{\mathrm{therm}}$ dataset. This way we obtain an uncertainty estimate of

17

0.035 ‰ due to thermal fractionation, leading to a total uncertainty on $\delta_{\text{grav}}$ of 0.04 ‰.

**2) Simplification of firn air transport**. We have simplified the DF calculation by assuming no fractionation occurs in the LIZ (Eq. 3). From the absence of gravitational separation we can conclude that advection (and perhaps dispersive mixing) must dominate LIZ gas transport, yet we cannot exclude the existence of a small diffusive flux. Indeed, some firn air models find that trace gas isotopes continue to be fractionated diffusively in the LIZ (Fig 1). We use the firn air model disagreement of 15% as an estimate of the uncertainty in the transport description.

**3) The age parameterization of Eq. (5)**. Our gas age parameterization provides a good fit to the modeled ages, with a coefficient of determination $R^2 = 0.94$. Antarctic glacial conditions lie outside the climatic range of modern day firn sites on which the parameterization is based. In particular, the hypothesis of a deepened convective zone during Antarctic glacial conditions may significantly influence the firn transport properties (Landais et al., 2006). However, the CZ thickness has very limited impact on $\Gamma(z_{\text{lid}})$, as we argued earlier in section 3. Our parameterization works very well for the deep convection Megadunes site, which has been proposed as a modern analog for glacial conditions on the Antarctic plateau (Severinghaus et al., 2010). For the offset from the linear fit in Fig. 2 we find a $1\sigma$ standard deviation of 1.8 years. With characteristic $CH_4$ ages of around 12 years, this corresponds to a relative error of 15 %.

Using standard error propagation methods, and assuming all errors to be uncorrelated, we find that the relative error in our method remains below

0.3 (i.e. 30%) in $\varepsilon_{\mathrm{DF}}$, at a typical value $\delta^{15}\mathrm{N{-}N_2} = 0.4$ ‰. Because the DCH is squared in the calculation, its uncertainty contributes most to the final error. If more accurate DCH estimates are available (from either heat diffusion modeling or additional $\delta^{40}\mathrm{Ar}$ or $\delta\mathrm{Kr/Ar}$ data) the uncertainty in the methed reduces to below 25%. Relative uncertainties for $CO_2$ isotopes will be slightly smaller because the air is older (smaller relative uncertainty in point 3 of our analysis).

## 5.2. Comparison to a firn densification / firn air transport modeling

The alternative to our DF correction method is a full modeling study, which combines heat diffusion, firn densification and firn air transport modeling. This approach will be superior or equal to our method on point 1 of our uncertainty analysis (section 5.1), as it will provide an accurate DCH estimate. Both our method and the modeling approach suffer the same uncertainty due to poorly understood LIZ transport (point 2). However, a full modeling approach is subject to many other uncertainties that do not affect our method. We list them below, without attempting to estimate their magnitude.

First, the firn densification model requires past accumulation and temperature estimates as an input, both of which have their uncertainty. Second, there is an inherent uncertainty to the densification modeling; e.g. different models can produce close-off depth values that differ by several meters. For Antarctic plateau glacial conditions, densification models systematically predict a deepening of the firn column, whereas $\delta^{15}\mathrm{N{-}N_2}$ data show a shortening of the DCH (Landais et al., 2006). The hypothesis of a deepened glacial CZ

is often invoked to explain this mismatch, which would require CZ thickness of up to 40 m at Dome Fuji (Severinghaus et al., 2010). Third, the close-off and lock-in depths need to be estimated from the density profile. The former is estimated using the parameterization by Martinerie et al. (1994), which is often (slightly) in disagreement with field data from firn sampling campaigns; the latter is often estimated by the ad-hoc assumption that the lock-in density simply lies 14 $\mathrm{kg\,m^{-3}}$ below the close-off density (Schwander et al., 1997; Blunier and Schwander, 2000). Fourth, the effective diffusivity-depth relationship is generally unknown. The best available parameterization by (Schwander, 1989) often gives unsatisfactory results to field data. Fifth, a full modeling study would require the true atmospheric mixing ratios as an input; these are unknown because the ice core contains a smooth version of the atmospheric signal due to firn diffusion and bubble trapping. The rapid variations that cause the strongest DF are attenuated in the firn, which act as a low-pass filter (Spahni et al., 2003; Köhler et al., 2011). By contrast, our semi-empirical method conveniently uses the mixing ratios as recorded in the ice core as an input.

Considering the above we contend that, compared to a full model approach, our DF correction method is certainly more accurate whenever good DCH estimates are available, and probably more accurate whenever the DCH is based directly on $\delta^{15}\mathrm{N}$–$\mathrm{N_2}$ data uncorrected for thermal fractionation.

## 6. Summary and conclusions

Fist, we derived an analytical expression for diffusive isotopic fractionation in the firn column. Second, based on data from ten firn air sites, we

20

derived a parameterization of the mean gas age at the lock-in depth. By combining both results, we obtain a convenient framework for correcting ice core data for the effect of diffusive fractionation. The gas age parameterization can also be used in $\Delta$age calculations.

We verified the accuracy and dynamic response of our method by comparing it to a firn air transport model for two modern, well-characterized firn air sites. We apply our method to $CH_4$, $CO_2$ and $N_2O$ mixing ratios found in ice cores. We find that $\delta^{13}C$–$CH_4$ is the only trace gas isotopic signal for which the diffusive correction should always be applied during transitions. Also, for the recent anthropogenic increase, isotopic data for all three trace gases needs to be DF corrected. In all other cases the effects of DF can usually be neglected.

We apply the DF correction to published $\delta^{13}C$–$CH_4$ records over the last glacial termination and the 8.2 ka event. In both cases the DF correction exceeds the analytical precision of the data during abrupt transitions, and has a significant impact on the observed isotopic trends.

We show that our method has an uncertainty of around 25% for typical Antarctic sites, as well as Greenland sites where thermal fractionation-corrected $\delta^{15}N$–$N_2$ data are used. For Greenland sites we estimate an uncertainty of around 30% when uncorrected $\delta^{15}N$–$N_2$ data are used. We argue that our method is more accurate than the alternative of a full modeling study.

Our method requires little computational effort and only commonly available ice core data. It offers a convenient and accurate framework for correcting ice core data for the effect of diffusive fractionation. In cases where the

fractionation is small, our method can provide a justification for neglecting the DF correction.

**References**

Alley, R.B., Ágústsdóttir, A.M., 2005. The 8k event: cause and consequences of a major holocene abrupt climate change. Quaternary Sci. Rev. 24, 1123 – 1149.

Atlas, E., Barnola, J.M., Bernard, S., Brenninkmeijer, C., Etheridge, D., Fraser, P., Mak, J., Mason-Delmotte, V., Mulvaney, R., Penkett, M., Röckmann, T., Schwander, J., Shine, K., Stroud, V., Sturges, W., Sturrock, G., a. CRYOspheric STudies of Atmospheric Trends in stratospherically and radiatively important gases (CRYOSTAT), last accessed 5 June 2012. `http://badc.nerc.ac.uk/view/badc.nerc.ac.uk__ATOM_ _dataent_cryostat`.

Atlas, E., Barnola, J.M., Brenninkmeijer, C., Mulvaney, R., Schwander, J., Sturges, W., Penkett, M., Penkett, S., Chappellaz, J., Jouzel, J., b. Firn Record of Trace Gases Relevant to Atmospheric Chemical Change over 100 yrs (FIRETRACC/100), last accessed 5 June 2012. `http://badc.nerc.ac.uk/view/badc.nerc.ac.uk__ATOM__dataent_FIRETRACC`.

Barnola, J.M., Pimienta, P., Raynaud, D., Korotkevich, Y.S., 1991. $CO_2$-climate relationship as deduced from the Vostok ice core - A reexamination based on new measurements and on a reevaluation of the air dating. Tellus B 43, 83–90.

Battle, M., Bender, M., Sowers, T., Tans, P.P., Butler, J.H., Elkins, J.W., Ellis, J.T., Conway, T., Zhang, N., Lang, P., Clarket, A.D., 1996. Atmospheric gas concentrations over the past century measured in air from firn at the south pole. Nature 383, 231–235.

Battle, M.O., Severinghaus, J.P., Sofen, E.D., Plotkin, D., Orsi, A.J., Aydin, M., Montzka, S.A., Sowers, T., Tans, P.P., 2011. Controls on the movement and composition of firn air at the West Antarctic Ice Sheet Divide. Atmos. Chem. Phys. 11, 11007–11021.

Blunier, T., Schwander, J., 2000. Gas enclosure in ice: age difference and fractionation. Hokkaido University Press, Sapporo. pp. 307–326.

Blunier, T., Spahni, R., Barnola, J.M., Chappellaz, J., Loulergue, L., Schwander, J., 2007. Synchronization of ice core records via atmospheric gases. Clim. Past 3, 325–330.

Bock, M., Schmitt, J., Behrens, M., Moller, L., Schneider, R., Sapart, C., Fischer, H., 2010a. A gas chromatography/pyrolysis/isotope ratio mass spectrometry system for high-precision delta D measurements of atmospheric methane extracted from ice cores. Rapid Commun. Mass Sp. 24, 621–633.

Bock, M., Schmitt, J., Moller, L., Spahni, R., Blunier, T., Fischer, H., 2010b. Hydrogen Isotopes Preclude Marine Hydrate $CH_4$ Emissions at the Onset of Dansgaard-Oeschger Events. Science 328, 1686–1689.

Buizert, C., Martinerie, P., Petrenko, V.V., Severinghaus, J.P., Trudinger, C.M., Witrant, E., Rosen, J.L., Orsi, A.J., Rubino, M., Etheridge, D.M., Steele, L.P., Hogan, C., Laube, J.C., Sturges, W.T., Levchenko, V.A., Smith, A.M., Levin, I., Conway, T.J., Dlugokencky, E.J., Lang, P.M., Kawamura, K., Jenk, T.M., White, J.W.C., Sowers, T., Schwander, J., Blunier, T., 2012. Gas transport in firn: multiple-tracer characterisation and model intercomparison for NEEM, Northern Greenland. Atmos. Chem. Phys. 12, 4259–4277.

Dreyfus, G.B., Jouzel, J., Bender, M.L., Landais, A., Masson-Delmotte, V., Leuenberger, M., 2010. Firn processes and $\delta^{15}N$: potential for a gas-phase climate proxy. Quaternary Sci. Rev. 29, 28–42.

EPICA community members, 2006. One-to-one coupling of glacial climate variability in Greenland and Antarctica. Nature 444, 195–198.

Etheridge, D.M., Steele, L.P., Langenfelds, R.L., Francey, R.J., Barnola, J.M., Morgan, V.I., 1996. Natural and anthropogenic changes in atmo-

spheric $CO_2$ over the last 1000 years from air in Antarctic ice and firn. J. Geophys. Res. 101, 4115–4128.

Fabre, A., Barnola, J.M., Arnaud, L., Chappellaz, J., 2000. Determination of gas diffusivity in polar firn: Comparison between experimental measurements and inverse modeling. Geophys. Res. Lett. 27, 557–560.

Fischer, H., Behrens, M., Bock, M., Richter, U., Schmitt, J., Loulergue, L., Chappellaz, J., Spahni, R., Blunier, T., Leuenberger, M., Stocker, T.F., 2008. Changing boreal methane sources and constant biomass burning during the last termination. Nature 452, 864–867.

Francey, R., Allison, C., Etheridge, D., Trudinger, C., Enting, I., Leuenberger, M., Langenfelds, R., Michel, E., Steele, L., 1999. A 1000-year high precision record of delta C-13 in atmospheric $CO_2$. Tellus B 51, 170–193.

Freitag, J., Dorbrindt, U., Kipfstuhl, J., 2002. A new method for predicting transport properties of polar firn with respect to gases on the pore-space scale. Ann. Glaciol. 35, 538–544. Doi:10.3189/172756402781816582.

Goujon, C., Barnola, J.M., Ritz, C., 2003. Modeling the densification of polar firn including heat diffusion: Application to close-off characteristics and gas isotopic fractionation for Antarctica and Greenland sites. J. Geophys. Res.-Atm 108, 18.

Huber, C., Leuenberger, M., Spahni, R., Fluckiger, J., Schwander, J., Stocker, T., Johnsen, S., Landals, A., Jouzel, J., 2006. Isotope calibrated Greenland temperature record over Marine Isotope Stage 3 and its relation to $CH_4$. Earth Planet. Sc. Lett. 243, 504–519.

Ishijima, K., Sugawara, S., Kawamura, K., Hashida, G., Morimoto, S., Murayama, S., Aoki, S., Nakazawa, T., 2007. Temporal variations of the atmospheric nitrous oxide concentration and its $\delta^{15}$N and $\delta^{18}$O for the latter half of the 20th century reconstructed from firn air analyses. J. Geophys. Res.-Atm 112, 12.

Kobashi, T., Severinghaus, J.P., Brook, E.J., Barnola, J.M., Grachev, A.M., 2007. Precise timing and characterization of abrupt climate change 8200 years ago from air trapped in polar ice. Quat. Sci. Rev. 26, 1212–1222.

Köhler, P., Knorr, G., Buiron, D., Lourantou, A., Chappellaz, J., 2011. Abrupt rise in atmospheric $CO_2$ at the onset of the Bølling/Allerød: in-situ ice core data versus true atmospheric signals. Clim. Past. 7, 473–486.

Landais, A., Barnola, J.M., Kawamura, K., Caillon, N., Delmotte, M., Van Ommen, T., Dreyfus, G., Jouzel, J., Masson-Delmotte, V., Minster, B., Freitag, J., Leuenberger, M., Schwander, J., Huber, C., Etheridge, D., Morgan, V., 2006. Firn-air delta N-15 in modern polar sites and glacial-interglacial ice: a model-data mismatch during glacial periods in Antarctica? Quaternary Sci. Rev. 25, 49–62.

Landais, A., Caillon, N., Goujon, C., Grachev, A.M., Barnola, J.M., Chappellaz, J., Jouzel, J., Masson-Delmotte, V., Leuenberger, M., 2004. Quantification of rapid temperature change during do event 12 and phasing with methane inferred from air isotopic measurements. Earth Planet. Sc. Lett. 225, 221–232.

Leuenberger, M.C., Lang, C., Schwander, J., 1999. Delta(15)N measurements

as a calibration tool for the paleothermometer and gas-ice age differences: A case study for the 8200 BP event on GRIP ice. J. Geophys. Res.-Atm 104, 22163–22170.

Loulergue, L., Schilt, A., Spahni, R., Masson-Delmotte, V., Blunier, T., Lemieux, B., Barnola, J.M., Raynaud, D., Stocker, T.F., Chappellaz, J., 2008. Orbital and millennial-scale features of atmospheric $CH_4$ over the past 800,000 years. Nature 453, 383–386.

Lourantou, A., Chappellaz, J., Barnola, J.M., Masson-Delmotte, V., Raynaud, D., 2010. Changes in atmospheric $CO_2$ and its carbon isotopic ratio during the penultimate deglaciation. Quaternary Sci. Rev. 29, 1983–1992. Doi: DOI: 10.1016/j.quascirev.2010.05.002.

Lüthi, D., Le Floch, M., Bereiter, B., Blunier, T., Barnola, J.M., Siegenthaler, U., Raynaud, D., Jouzel, J., Fischer, H., Kawamura, K., Stocker, T.F., 2008. High-resolution carbon dioxide concentration record 650,000-800,000 years before present. Nature 453, 379–382.

Martinerie, P., Lipenkov, V.Y., Raynaud, D., Chappellaz, J., Barkov, N.I., Lorius, C., 1994. Air content paleo record in the vostok ice core (antarctica): A mixed record of climatic and glaciological parameters. J. Geophys. Res. 99, 10565–10576.

McManus, J.F., Francois, R., Gherardi, J.M., Keigwin, L.D., Brown-Leger, S., 2004. Collapse and rapid resumption of atlantic meridional circulation linked to deglacial climate changes. Nature 428, 834–837.

Melton, J.R., Schaefer, H., Whiticar, M.J., 2012. Enrichment in $^{13}$C of atmospheric $CH_4$ during the Younger Dryas termination. Clim. Past 8, 1177–1197.

Mischler, J.A., Sowers, T.A., Alley, R.B., Battle, M., McConnell, J.R., Mitchell, L., Popp, T., Sofen, E., Spencer, M.K., 2009. Carbon and hydrogen isotopic composition of methane over the last 1000 years. Global Biogeochem. Cy. 23.

NGRIP community members, 2004. High-resolution record of Northern Hemisphere climate extending into the last interglacial period. Nature 431, 147–151.

Rommelaere, V., Arnaud, L., Barnola, J.M., 1997. Reconstructing recent atmospheric trace gas concentrations from polar firn and bubbly ice data by inverse methods. J. Geophys. Res.-Atm 102, 30069–30083.

Sapart, C.J., van der Veen, C., Vigano, I., Brass, M., van de Wal, R.S.W., Bock, M., Fischer, H., Sowers, T., Buizert, C., Sperlich, P., Blunier, T., Behrens, M., Schmitt, J., Seth, B., Röckmann, T., 2011. Simultaneous stable isotope analysis of methane and nitrous oxide on ice core samples. Atmos. Meas. Tech. 4, 2607–2618.

Schilt, A., Baumgartner, M., Blunier, T., Schwander, J., Spahni, R., Fischer, H., Stocker, T.F., 2010. Glacialial–interglacial and millennial-scale variations in the atmospheric nitrous oxide concentration during the last 800,000 years. Quaternary Sci. Rev. 29, 182 – 192.

Schmitt, J., Schneider, R., Elsig, J., Leuenberger, D., Lourantou, A., Chappellaz, J., Köhler, P., Joos, F., Stocker, T.F., Leuenberger, M., Fischer, H., 2012. Carbon Isotope Constraints on the Deglacial $CO_2$ Rise from Ice Cores. Science 336, 711–714.

Schüpbach, S., Federer, U., Kaufmann, P.R., Hutterli, M.A., Buiron, D., Blunier, T., Fischer, H., Stocker, T.F., 2009. A New Method for High-Resolution Methane Measurements on Polar Ice Cores Using Continuous Flow Analysis. Environ. Sci. Technol. 43, 5371–5376.

Schwander, J., 1989. The transformation of snow to ice and the occlusion of gases, in: Oescher, H., Langway, C. (Eds.), The Environmental record in glaciers and ice sheets. John Wiley, New York, pp. 53–67.

Schwander, J., Sowers, T., Barnola, J.M., Blunier, T., Fuchs, A., Malaize, B., 1997. Age scale of the air in the Summit ice: Implication for glacial-interglacial temperature change. J. Geophys. Res.-Atm 102, 19483–19493.

Schwander, J., Stauffer, B., Sigg, A., 1988. Air mixing in firn and the age of the air at pore close-off. Ann. Glaciol. 10, 141–145.

Severinghaus, J.P., Albert, M.R., Courville, Z.R., Fahnestock, M.A., Kawamura, K., Montzka, S.A., Muhle, J., Scambos, T.A., Shields, E., Shuman, C.A., Suwa, M., Tans, P., Weiss, R.F., 2010. Deep air convection in the firn at a zero-accumulation site, central Antarctica. Earth Planet Sci. Lett. 293, 359–367.

Severinghaus, J.P., Brook, E.J., 1999. Abrupt climate change at the end of

the last glacial period inferred from trapped air in polar ice. Science 286, 930–934.

Severinghaus, J.P., Grachev, A., Battle, M., 2001. Thermal fractionation of air in polar firn by seasonal temperature gradients. Geochem. Geophy. Geosy. 2.

Sowers, T., 2006. Late Quaternary Atmospheric $CH_4$ Isotope Record Suggests Marine Clathrates Are Stable. Science 311, 838–840.

Sowers, T., 2010. Atmospheric methane isotope records covering the holocene period. Quaternary Sci. Rev. 29, 213–221. DOI: 10.1016/j.quascirev.2009.05.023.

Sowers, T., Alley, R.B., Jubenville, J., 2003. Ice Core Records of Atmospheric $N_2O$ Covering the Last 106,000 Years. Science 301, 945–948.

Spahni, R., Schwander, J., Flückiger, J., Stauffer, B., Chappellaz, J., Raynaud, D., 2003. The attenuation of fast atmospheric $CH_4$ variations recorded in polar ice cores. Geophys. Res. Lett. 30, 1571.

Stowasser, C., Buizert, C., Gkinis, V., Chappellaz, J., Schüpbach, S., Bigler, M., Fain, X., Sperlich, P., Baumgartner, M., Schilt, A., Blunier, T., 2012. Continuous measurements of methane mixing ratios from ice cores. Atmos. Meas. Tech. 5, 999–1013.

Sturrock, G.A., Etheridge, D.M., Trudinger, C.M., Fraser, P.J., Smith, A.M., 2002. Atmospheric histories of halocarbons from analysis of antarctic firn air: Major montreal protocol species. J. Geophys. Res.-Atm 107, 14.

Trudinger, C.M., Enting, I.G., Etheridge, D.M., Francey, R.J., Levchenko, V.A., Steele, L.P., Raynaud, D., Arnaud, L., 1997. Modeling air movement and bubble trapping in firn. J. Geophys. Res.-Atm 102, 6747–6763.

Witrant, E., Martinerie, P., Hogan, C., Laube, J.C., Kawamura, K., Capron, E., Montzka, S.A., Dlugokencky, E.J., Etheridge, D., Blunier, T., Sturges, W.T., 2011. A new multi-gas constrained model of trace gas non-homogeneous transport in firn: evaluation and behavior at eleven polar sites. Atmos. Chem. Phys. Discuss. 11, 23029–23080.

Table 1: Diffusivity ratios of isotopologues following Buizert et al. (2012) (second column) and Trudinger et al. (1997) (third column); trace gas diffusivity relative to $CO_2$ at -30°C for use in Eq. (4) (fourth column).

| | $\left(\frac{D}{D_i} - 1\right)$ | $\left(\frac{D}{D_i} - 1\right)$ | $\gamma_X$ |
|---|---|---|---|
| HH/HD | $20.50 \cdot 10^{-2}$ | - | 4.694 |
| $^{12}CH_4/^{13}CH_4$ | $1.95 \cdot 10^{-2}$ | $1.79 \cdot 10^{-2}$ | 1.367 |
| $CH_4/CH_3D$ | $1.96 \cdot 10^{-2}$ | - | 1.367 |
| $^{12}CO/^{13}CO$ | $0.89 \cdot 10^{-2}$ | - | 1.250 |
| $C^{16}O/C^{18}O$ | $1.74 \cdot 10^{-2}$ | - | 1.250 |
| $^{12}CO_2/^{13}CO_2$ | $0.44 \cdot 10^{-2}$ | $0.42 \cdot 10^{-2}$ | 1.000 |
| $C^{16}O^{16}O/C^{18}O^{16}O$ | $0.88 \cdot 10^{-2}$ | - | 1.000 |
| $^{14}N^{14}NO/^{15}N^{14}NO$ | $0.44 \cdot 10^{-2}$ | - | 0.981 |
| $NN^{16}O/NN^{18}O$ | $0.88 \cdot 10^{-2}$ | - | 0.981 |

Table 2: Overview of firn air sites used in the gas age parameterization.

| Site | $p$ | $T$ | $A$ | DCH |
|---|---|---|---|---|
| | (hPa) | (°C) | (m ice a$^{-1}$) | (m) |
| Berkner Island | 895 | -26 | 0.13 | 52 |
| DE08-2 | 850 | -19 | 1.20 | 67 |
| Dome C | 658 | -54 | 0.032 | 93 |
| DSSW20K | 850 | -21 | 0.16 | 42 |
| Megadunes | 677 | -49 | 0.025[a] | 35 |
| South Pole | 681 | -51 | 0.08 | 114 |
| WAIS-Divide | 780 | -31 | 0.22 | 63 |
| NEEM | 745 | -28.9 | 0.22 | 60 |
| NGRIP | 691 | -31.1 | 0.19 | 66 |
| Summit | 665 | -31.4 | 0.23 | 67 |

[a] Long term average. Current value close to zero.

Table 3: Typical magnitude of $\varepsilon_{\mathrm{DF}}$ and measurement precision; results from Greenland and EDC are combined. The columns give typical $\varepsilon_{\mathrm{DF}}$ values for trace gas increases in the recent anthropogenic era (during maximum increase), over the glacial terminations $\mathrm{T}_I$–$\mathrm{T}_{III}$, and over Dansgaard-Oeschger (DO) cycles. The last column lists the reported range of ice core measurement precision.

| | max $\varepsilon_{\mathrm{DF}}$ Anthr. (‰) | $\varepsilon_{\mathrm{DF}}$ $\mathrm{T_{I-III}}$ (‰) | $\varepsilon_{\mathrm{DF}}$ DO (‰) | Analytical (‰) |
|---|---|---|---|---|
| $\delta^{13}$C–CH$_4$ | $1.2^a$ | 0.4–1.0 | 0.2–0.4 | $0.15$–$0.3^{a,b,c}$ |
| $\delta$D–CH$_4$ | $1.2^a$ | 0.4–1.0 | 0.2–0.4 | $2.1$–$4.2^{b,d,e}$ |
| $\delta^{13}$C–CO$_2$ | $0.12^f$ | 0.01–0.017 | $< 0.005$ | $0.016$–$0.1^{g,h,i,j}$ |
| $\delta^{15}$N–N$_2$O | $0.12^k$ | 0.01–0.03 | 0.005–0.018 | $0.5^{b,l}$ |
| $\delta^{18}$O–N$_2$O | $0.24^l$ | 0.02–0.06 | 0.01–0.035 | $0.69$–$2^{b,l}$ |

[a] Mischler et al. (2009)

[b] Sapart et al. (2011)

[c] Fischer et al. (2008)

[d] Sowers (2006)

[e] Bock et al. (2010a)

[f] Modern day Law Dome, Trudinger et al. (1997)

[g] Francey et al. (1999)

[h] Lourantou et al. (2010)

[i] Schmitt et al. (2012)

[j] T. Bauska, personal communication, 2012

[k] Modern day NGRIP Ishijima et al. (2007)
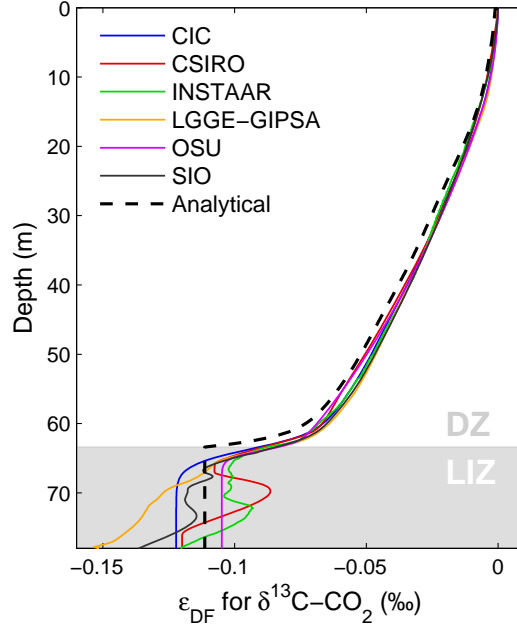
[l] Sowers et al. (2003)

Figure 1: Isotopic diffusive fractionation at NEEM for a hypothetical atmospheric scenario $[CO_2] = 225 \exp\left[2.5 \cdot 10^{-3}(t - 1800)\right]$, with $t$ the time in calendar years. The scenario corresponds to a constant $k/C = 2.5 \times 10^{-3}$ a$^{-1}$. Model acronyms and details are given in Buizert et al. (2012). $\Gamma(z)$ is calculated using the CIC firn air model. DZ and LIZ are indicated by changes in shading.
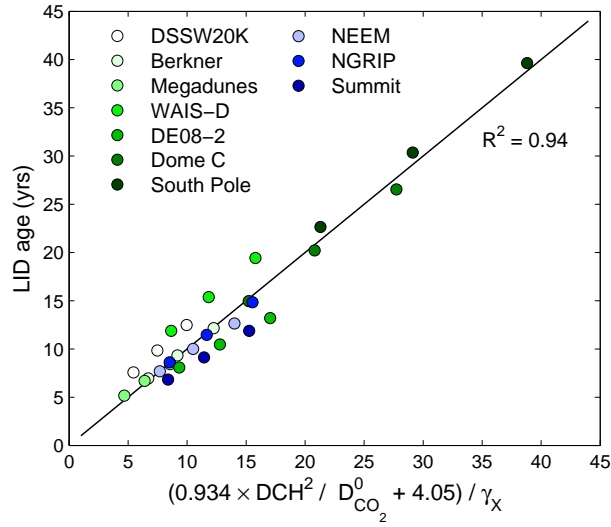
Figure 2: Gas age at the lock-in depth ($z_{\mathrm{lid}}$) for 10 different firn air sites, and three different gases ($CH_4$, $CO_2$ and one hypothetical, with $\gamma_{CH_4} = 1.367$, $\gamma_{CO_2} = 1$ and $\gamma_X = 0.75$). Three points at each site represent the three gases, with $CH_4$ being the youngest, and the hypothetical gas the oldest. The Lock-in depth is defined as the depth where the effective molecular diffusivity is reduced to $D_X(z_{\mathrm{lid}}) = D_X^0/1000$. The diffusive column height (DCH) is derived from the $\delta^{15}N$–$N_2$ in the LIZ, $DCH = \ln\left(\delta^{15}N/10^3 + 1\right) \times RT/\Delta Mg$.
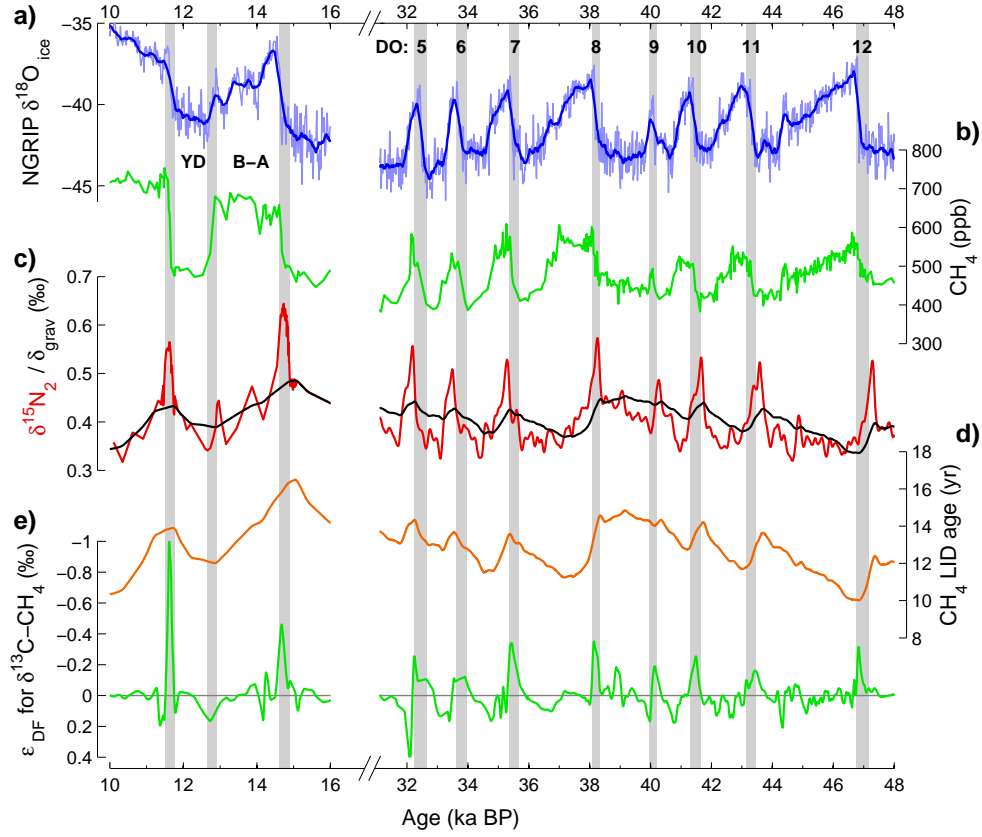
Figure 3: Diffusive isotopic fractionation for $CH_4$ in Greenland. Ages are before the year 1950 C.E. (BP). **a)** Precipitation $\delta^{18}O$ as a proxy for site temperature from the NGRIP ice core on the GICC05 time scale (NGRIP community members, 2004). **b)** Composite record of northern hemisphere $CH_4$ mixing ratio based on GRIP, GISP2 and NGRIP ice core samples (Blunier et al., 2007). **c)** Measured $\delta^{15}N$ (in red) from NGRIP (30–48 ka BP; Huber et al., 2006) and GISP2 (10–16 ka BP, Severinghaus and Brook, 1999), and modeled gravitational signal $\delta_{grav}$ (in black) for NGRIP (30–48 ka BP, modeled; Huber et al., 2006) and GISP2 (10–16 ka BP, estimated by eye). **d)** Calculated age $\Gamma(z_{lid})$ using Eq. (5) based on $\delta_{grav}$. **e)** Spline fit to calculated DF signal $\varepsilon_{DF}$ from Eq. (2).
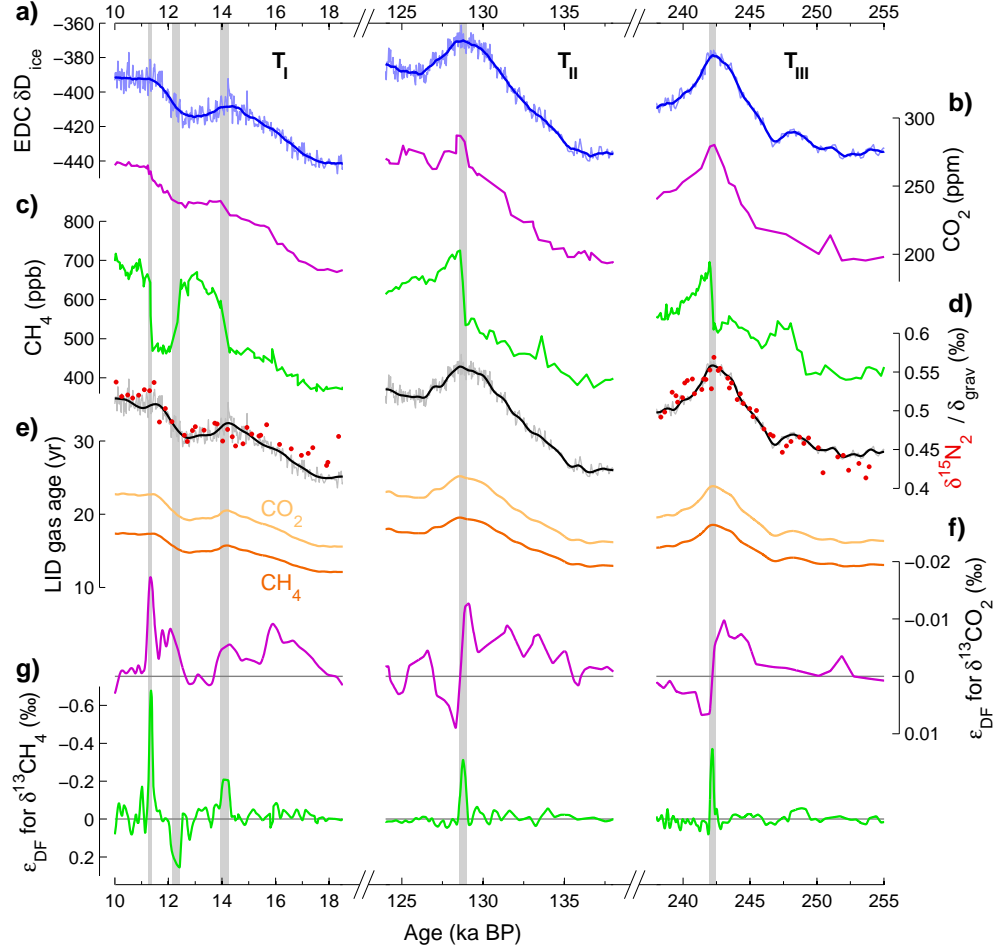
.

Figure 4: Diffusive isotopic fractionation for $CH_4$ and $CO_2$ in the EPICA Dome C ice core, Antarctica. Ages are before the year 1950 C.E. (BP). **a)** Precipitation $\delta D$ as a proxy for site temperature on the EDC-3 timescale. **b)** $CO_2$ mixing ratio from EDC and Vostok ice core samples (Lüthi et al., 2008). **c)** $CH_4$ mixing ratio from EDC ice core samples (Loulergue et al., 2008). **d)** Measured $\delta^{15}N$ (in red) and $\delta_{grav}$ (in black) from the $\delta^{15}N$-$\delta D$ relationship from Dreyfus et al. (2010); for $T_{III}$ an ad-hoc 0.02 ‰ was added to improve the fit. **e)** Calculated age $\Gamma(z_{lid})$ using Eq. (5) based on $\delta_{grav}$. **f)** Spline fit to calculated $CO_2$ DF signal $\varepsilon_{DF}$ from Eq. (2). **g)** Spline fit to calculated $CH_4$ DF signal. Values for $N_2O$ isotopologues (Table 3) were calculated in the same way as for $CO_2$ and $CH_4$, using the EPICA Dome C $N_2O$ mixing ratios by Schilt et al. (2010).
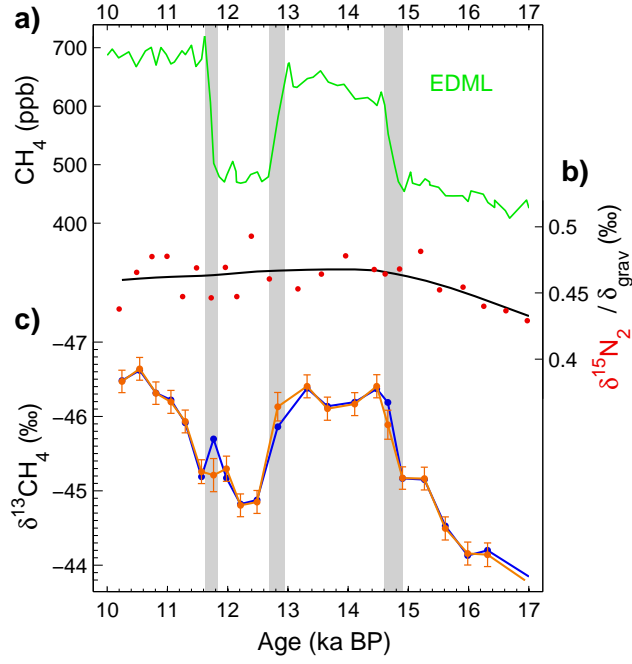
38

Figure 5: DF correction of $\delta^{13}$C–CH$_4$ data over the last glacial termination. Ages are before the year 1950 C.E. (BP). **a)** EDML CH$_4$ data from EPICA community members (2006). **b)** $\delta_{\mathrm{grav}}$ (black) from Fischer et al. (2008) and $\delta^{15}$N–N$_2$ data (red) from A. Landais (personal communication, 2011). **c)** $\delta^{13}$C–CH$_4$ data from Fischer et al. (2008) before (blue), and after DF correction (orange, with error bars). DF-correction based on black $\delta_{\mathrm{grav}}$ curve. Note that the isotopic scale has been inverted.
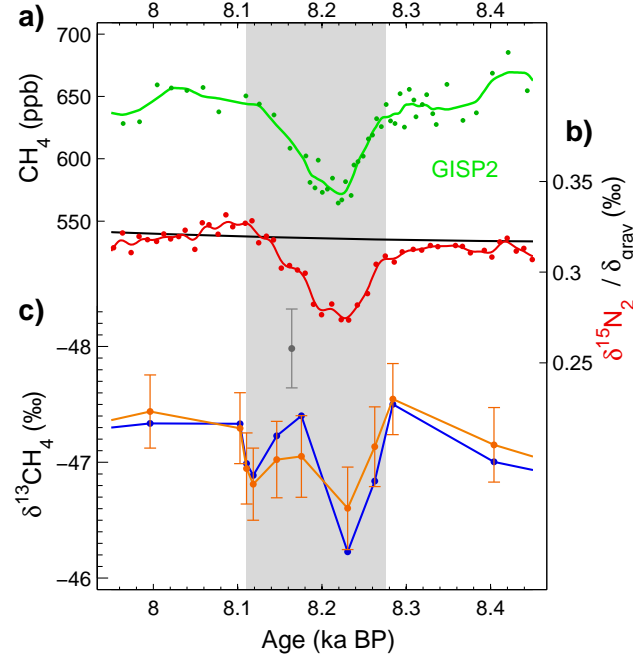
Figure 6: DF correction of $\delta^{13}$C–CH$_4$ data over the 8.2 ka event. Ages are before the year 1950 C.E. (BP). **a)** High resolution GISP2 CH$_4$ and **b)** $\delta^{15}$N–N$_2$ data from Kobashi et al. (2007). The plotted $\delta_{\mathrm{grav}}$ signal (in black) is a quadratic fit to the reconstructed $\delta_{\mathrm{grav}}$ based on $\delta^{15}$N$_{\mathrm{excess}} = \delta^{15}$N$-\delta^{40}$Ar/4. **c)** $\delta^{13}$C–CH$_4$ data from Sowers (2010) before (blue), and after DF correction (orange, with error bars). DF-correction based on black $\delta_{\mathrm{grav}}$ curve. Note that the isotopic scale has been inverted.